Synthesis of the New One-Dimensional Compound Sr_3NiPtO_6: Structure and Magnetic Properties

T. N. Nguyen, D. M. Giaquinta, and H.-C. zur Loye*

Department of Chemistry, Massachusetts Institute of Technology, Cambridge, Massachusetts 02139

Received January 19, 1994. Revised Manuscript Received June 28, 1994[⊗]

Single crystals of a new one-dimensional oxide, Sr_3NiPtO_6, containing Ni(II) in an usual trigonal prismatic coordination were synthesized electrochemically using platinum electrodes in a mixture of $SrCO_3$ and NiO dissolved in a KOH flux. Since the as-grown crystals were twinned, the structure was determined by Rietveld analysis of the X-ray and neutron powder data. The structure was refined in space group $R\bar{3}c$, with $a = 9.5832(1)$ and $c = 11.1964(1)$. Sr_3NiPtO_6, structurally related to Sr_3CuPtO_6 and the parent compound A_4PtO_6 (A = Ca, Sr,Ba), contains infinite chains of alternating, face-sharing PtO_6 octahedra and NiO_6 trigonal prisms. Magnetic susceptibility studies of Sr_3NiPtO_6 indicate the presence of Ni(II) ions with large single-ion anisotropy ($D = 90.2$ K, $g = 2.37$, $\chi_{TIP} = 5.7 \times 10^{-4}$ emu/mol) and the onset of low-dimensional, short-range antiferromagnetic ordering at ~25 K. In contrast, Sr_3CuPtO_6 exhibits $S = {}^1/_2$ Heisenberg linear chain antiferromagnetism with $J/k = -26.1$ K and $\bar{g} = 2.21$.

Introduction

Electrosynthesis in molten salts is a well-known technique that has been used to synthesize many types of solid-state materials in single-crystal form.[1-6] The electrosynthesis technique offers numerous advantages, including access to unusual oxidation states, convenience of lower reaction temperatures, and fast reaction times, over conventional solid-state synthesis. Combined, these attributes can lead to single crystals of novel materials that may not be prepared by other synthetic routes. Much of the work done previously has concentrated on cathodic reactions and the synthesis of reduced early transition metal materials at temperatures often exceeding 800 °C.[1,7-11]

Recently, many new oxides containing high-valent late transition metals or bismuth have been synthesized in molten alkali hydroxides using the flux method.[12-22] A modification of the flux method by the addition of an electrochemical potential gradient as the active reaction driving force has lead to the synthesis of additional new compounds. Using electrochemistry, Norton was able to synthesize single crystals of the superconductor $(Ba,K)BiO_3$ at temperatures as low as 180 °C in molten KOH.[23] The mechanism of this reaction has also been investigated.[24] Similarly, we have prepared single crystals of the potassium ion conductor $KBiO_3$, a phase previously prepared only at high temperature and high oxygen pressure.[25] Hydroxide fluxes are promising as good solvents for the electrosynthesis of highly oxidized late transition metal materials. The hydroxides are low melting with low volatility and toxicity, and they readily dissolve many oxides. Furthermore, their well-studied Lux–Flood acid–base chemistry may help in the understanding of the electrosynthesis process. In this paper we report the electrosynthesis, structure, and magnetic properties of Sr_3NiPtO_6, a new $S = 1$ one-dimensional oxide. Chain systems with $S = 1$ have received much attention recently due to the possible

[⊗] Abstract published in *Advance ACS Abstracts,* August 15, 1994.

(1) Wold, A., Bellavance, D. In *Preparative Methods in Solid State Chemistry*; Hagenmuller, P., Ed.; Academic Press: New York, 1972; pp 279–308.
(2) Feigelson, R. S. In *Solid State Chemistry: A Contemporary Overview*; Robbins, M. H., Ed.; American Chemical Society: Washington, DC, 1980, Vol. 186, pp 243–275.
(3) Elwell, D. In *1976 Crystal Growth and Materials*; Kaldis, E., Scheel, H.J., Eds.; North-Holland Publishing Company: Amsterdam, 1977; pp 606–637.
(4) Elwell, D.; DeMattei, R. C.; Zubeck, I. V.; Feigelson, R. S.; Huggins, R. A. *J. Cryst. Growth* **1976**, *33*, 232–238.
(5) Crouch-Baker, S.; Huggins, R. A. *J. Mater. Res.* **1989**, *4*, 1495.
(6) Kunnmann, W. *A Review of the Preparation of Single Crystals by Fused Melt Electrolysis and Some General Properties*; Dekker: New York, 1971; Vol. 1, pp 1–36.
(7) Schneemeyer, L. F.; Spengler, S. E.; DiSalvo, F. J.; Waszcak, J. V. *Mater. Res. Bull.* **1984**, *19*, 525.
(8) Ravindran Nair, K.; Wang, E.; Greenblatt, M. *J. Solid State Chem.* **1984**, *55*, 193–199.
(9) Ramanujachary, K. V.; Greenblatt, M.; Jones, E. B.; McCarroll, W. H. *J. Solid State Chem.* **1993**, *102*, 69–78.
(10) Reid, A. F.; Watts, J. A. *J. Solid State Chem.* **1970**, *1*, 310–318.
(11) McCarroll, W. H.; Darling, C.; Jakubicki, G. *J. Solid State Chem.* **1983**, *48*, 189–195.
(12) Lee, J.; Holland, G. *J. Solid State Chem.* **1991**, *93*, 267–271.
(13) Carlson, V. A.; Stacy, A. M. *J. Solid State Chem.* **1992**, *96*, 332–343.
(14) Ham, W. K.; Holland, G. F.; Stacy, A. M. *J. Am. Chem. Soc.* **1988**, *110*, 5214–5215.
(15) Cava, R. J.; Siegrist, T.; Peck Jr., W. F.; Krajewski, J. J.; Batlogg, B.; Rosamilia, J. *Phys. Rev. B* **1991**, *44*, 9746–9748.
(16) Schneemeyer, L. F.; Thomas, J. K.; Siegrist, T.; Batlogg, B.; Rupp, L. W.; Opila, R. L.; Cava, R. J.; Murphy, D. W. *Nature* **1988**, *335*, 267.
(17) Wattiaux, A.; Fournes, L.; Demourgues, A.; Bernaben, N.; Grenier, J. C.; Pouchard, M. *Solid State Commun.* **1991**, *77*, 489.
(18) VerNooy, P. D.; Dixon, M.; Hollander, F.; Stacy, A. M. *Inorg. Chem.* **1990**, *29*, 2837–2841.
(19) Pickardt, J.; Paulus, W.; Schmalz, M.; Schöllhorn, R. *J. Solid State Chem.* **1990**, *89*, 308–314.
(20) Bezzenberger, R.; Schöllhorn, R. *Eur. J. Solid State Inorg. Chem.* **1993**, *30*, 435–445.
(21) Kodialam, S.; Korthius, V. C.; Hoffman, R.-D.; Sleight, A. W. *Mater. Res. Bull.* **1992**, *27*, 1379.
(22) VerNooy, P.; Stacy, A. M. *J. Solid State Chem.* **1991**, *95*, 270–274.
(23) Norton, M.; Tang, H.-Y. *Chem. Mater.* **1991**, *3*, 431–434.
(24) Roberts, G. L.; Kauzlarich, S. M.; Glass, R. S.; Estill, J. C. *Chem. Mater.* **1993**, *5*, 1645.
(25) Nguyen, T. N.; Giaquinta, D. M.; Davis, W.; zur Loye, H.-C. *Chem. Mater.* **1993**, *5*, 1273–1276.

0897-4756/94/2806-1642$04.50/0

existence of a Haldane gap.[26-28] For one-dimensional antiferromagnetic systems with integer spin, Haldane has predicted the existence of an energy gap between the nonmagnetic singlet ground state and the excited states,[29,30] whereas for a noninteger spin Heisenberg antiferromagnet, there is a continuum of excited states from the ground state without a gap. For comparison, we also report the magnetic properties of the isotypic Sr_3CuPtO_6 prepared via solid state synthesis. Wilkinson et. al. have prepared Sr_3CuPtO_6 via flux methods; however, no characterization of physical properties was reported.[31]

Experimental Section

Sample Preparation. Sr_3NiPtO_6 was synthesized by constant-potential, two-electrode electrolysis in molten KOH. A typical reaction mixture consisted of 0.7 g (4.75 mmol) of $SrCO_3$ (Cerac, 99.5%), 0.25 g (3.35 mmol) of NiO (Johnson Matthey, reagent grade), and 32 g (570 mmol) of KOH (Mallinckrodt, reagent grade). This mixture was placed in an alumina crucible and heated quickly to 700 °C. The reaction mixture was allowed to equilibrate at 700 °C for 4 h. Once equilibrated, two platinum electrodes (0.020 in. diameter) were inserted into the melt, and a constant potential of 0.65–0.7 V was applied. Control experiments in which no potential was applied did not yield any material. Slow cooling a mixture of $SrCO_3$, NiO, and Pt metal dissolved in molten KOH resulted in the crystallization of the known oxide, $Sr_5Ni_4O_{11}$.[12]

Electrolysis for approximately 12 h yielded single crystals of Sr_3NiPtO_6 on the platinum anode, while the platinum cathode was almost completely consumed. The crystals of Sr_3NiPtO_6 grew as dark brown to black hexagonal prisms as big as 0.2 × 1 mm. They were extracted with a probe and any residual flux was removed by washing with methanol. Replacing $SrCO_3$ with $Ca(OH)_2$ in the reaction mixture in order to make the Ca_3NiPtO_6 analog only produced Ca_4PtO_6, a known material structurally similar to Sr_3NiPtO_6. Switching to both palladium or nickel electrodes to make the nickel–palladium or the all-nickel analog, respectively, did not yield the desired products. The use of two palladium electrodes only resulted in the formation of NiO single crystals.

Polycrystalline samples of Sr_3NiPtO_6 and Sr_3CuPtO_6 were prepared via solid-state reactions. Stoichiometric amounts of $SrCO_3$, (Cerac, 99.5%), Pt metal (Aesar, 99.99%), and NiO (Cerac, 99.995%) or CuO (Cerac, 99.999%) were intimately mixed and pressed into pellets. The pellets were placed on platinum foil in alumina boats during heating to prevent contamination. Heating the samples at 1150 °C with intermittent grindings yielded single phase materials after 2 weeks.

Structural Characterization. Single-crystal composition was determined by wavelength-dispersive analysis using a JEOL 733 microprobe with internal standards. Powder samples were structurally characterized using a Rigaku RU300 X-ray diffractometer using Cu Kα radiation, λ = 1.5405 Å. A polycrystalline sample of Sr_3NiPtO_6 was used for the structure determination. An X-ray powder diffraction step scan was collected from 5 to 105° 2θ in steps of 0.01° 2θ using a collection time of 5 s/step. A Rietveld refinement of the powder X-ray diffraction data were performed using the refinement package GSAS[32] using the single-crystal structure of Sr_3CuPtO_6 as a starting model. Powder neutron diffraction data was collected at the NIST nuclear facility at Gaithersburg, MD. GSAS was also used to refine the neutron data scan taken from 7 to 120° 2θ with a step interval of 0.05°. The neutron wavelength was 1.5400 Å.

The oxygen content of the samples was determined by thermogravimetric analysis (TGA) using a Cahn TG121 system. Samples weighing approximately 50–100 mg were heated to 900 °C in 5% H_2/95% N_2. The initial oxygen content was back-calculated from the weight loss. Heating oxygen deficient samples in pure oxygen to 700 °C resulted in a weight gain associated with the complete oxidation of the compounds.

Magnetic Measurements. Magnetic measurements were obtained using a Quantum Design MPMS SQUID magnetometer at temperatures ranging from 2 to 300 K and in applied fields of 1, 5, and 40 kG. All samples were fully oxidized by annealing in O_2 at 550–750 °C before being used for any magnetic measurements. For data collection, all samples were cooled in zero field to 5 K. Once the sample temperature reached 5 K, the magnetic field was turned on and data were collected. All data were corrected for the diamagnetic contribution of the calibrated Kel-F sample container.

Results and Discussion

Structural Characterization. Precession photographs of Sr_3NiPtO_6 crystals revealed hexagonal symmetry with no obvious twinning. Attempts to refine the single-crystal structure in a hexagonal space group were not successful. Refining the structure in a rhombohedral space group, $R\bar{3}c$, and in the monoclinic space group, $C2/c$, of the isotypic Sr_3CuPtO_6 gave qualitatively similar structures with R = 6.1% and R = 5.5%, respectively. However, closer examination of the X-ray diffraction data showed systematic absences that were inconsistent with hexagonal, rhombohedral, or monoclinic symmetry, suggesting that the as-grown crystals of Sr_3NiPtO_6 are twinned. This observation is consistent with flux grown Sr_3CuPtO_6 which also exhibits twinning.[33] Furthermore, the relatively fast reaction time of electrolysis is often known to strain the reaction product and to produce defects.[4,34,35] Attempts to grow Sr_3NiPtO_6 at different temperatures and/or different deposition potentials produced no noticeable improvements.

The structure of Sr_3NiPtO_6 was subsequently refined by powder X-ray Rietveld analysis using the program GSAS; see Table 1. The powder samples of Sr_3NiPtO_6 prepared by solid-state reactions had an oxygen stoichiometry ranging from 5.9 to 6.0 as determined by thermogravimetric analysis. The oxygen content was a function of the cooling rate from high temperatures. Reactions in which the furnace was simply turned off from high temperatures gave the most oxygen-deficient materials; however, the samples can be fully oxidized by annealing in oxygen at 550–750 °C. Data collected for both oxygen-deficient and fully oxidized samples were used for Rietveld analysis. No structural differences were observable in the resultant structures indicating that the oxygen deficiencies must be random. The Rietveld refinement was carried out both in the space group of the parent compound, A_4PtO_6 (A = Ca, Sr, Ba) $R\bar{3}c$, and in that of the structurally related Sr_3CuPtO_6,

(26) Gadet, V.; Verdaguer, M.; Briois, V.; Gleizes, A.; Renard, J. P.; Beauvillain, P.; Chappert, C.; Goto, T.; Le Dang, K.; Veillet, P. *Phys. Rev. B* **1991**, *44*, 705.
(27) Renard, J. P.; Verdaguer, M.; Regnault, L. P.; Erkelens, W. A. C.; Rossat-Mignod, J.; Ribas, J.; Stirling, W. G.; Vettier, C. *J. Appl. Phys.* **1988**, *63*, 3538.
(28) Darriet, J.; Regnault, L. P. *Solid State Commun.* **1993**, *86*, 409.
(29) Haldane, F. D. M. *Phys. Rev. Lett.* **1983**, *50*, 1153.
(30) Haldane, F. D. M. *Phys. Lett.* **1983**, *93A*, 464.
(31) Wilkinson, A. P.; Cheetham, A. K.; Kunnman, W.; Kvick, A. *Eur. J. Solid State Inorg. Chem.* **1991**, *28*, 453–459.
(32) Larson, A. C.; von Dreele, R. B. In GSAS: General Structure Analysis System; Los Alamos National Laboratory: Los Alamos, NM, 1990.
(33) Hodeau, J. L.; Tu, H. Y.; Bordet, P.; Fournier, T.; Strobel, P.; Marezio, M.; Chandrashekar, G. V. *Acta Crystallogr.* **1992**, *B48*, 1–11.
(34) Zubeck, I. V.; Feigelson, R. S.; Huggins, R. A.; Pettit, P. A. *J. Cryst. Growth* **1976**, *34*, 85–91.
(35) Bostanov, V. *J. Cryst. Growth* **1977**, *42*, 194–200.

Table 1. Crystallographic Data for Sr_3NiPtO_6 at 25 °C

formula	Sr_3NiPtO_6
color	brownish-black crystals; light brown powder
formula weight	612.65
space group	$R\bar{3}c$ (No. 167)
a, Å	9.5832(1)
c, Å	11.1964(1)
V, Å^3	890.51
Z	6
D_{calc}, g/cm^3	6.792
λ, Å	Cu Kα X-ray, 1.5405
2θ scan range (deg)	5–105
step interval (deg 2θ)	0.01
maximum step intensity (counts)	66740
no. of unique reflections	216
no. of structural parameters[a]	7
no. of background parameters	6
no. of profile parameters	6
refinement	Rietveld using GSAS[b] with pseudo-Voigt[c] peak shape function
R_{wp}[d]	0.146
R_p[e]	0.108
χ^2	21.39

[a] Includes atomic positional and displacement parameters and unit-cell dimensions. [b] General Structure Analysis System, LANSCE, Los Alamos National Laboratory. [c] *J. Appl. Crystallogr.* **1982**, *15*, 615–620. [d] $R_{wp} = [\sum w(I_o - I_c)^2/\sum w I_o^2]$. [e] $R_p = \sum|I_o - I_c|/\sum I_o$, where I_o and I_c are the observed and calculated integrated intensities, respectively, and w is the weight derived from an error propagation scheme during the least-squares refinement process.

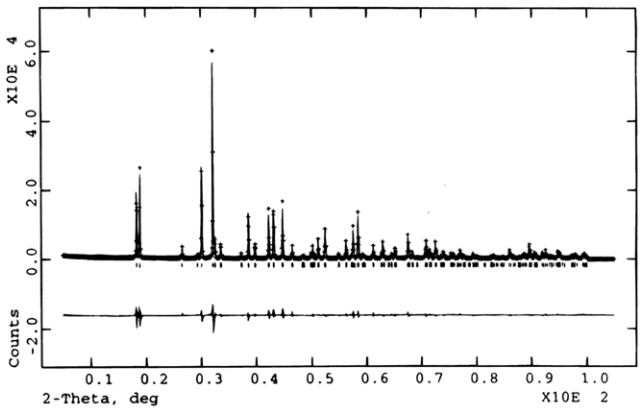

Figure 1. Rietveld analysis of the X-ray powder data for Sr_3NiPtO_6 showing the observed, calculated, and difference patterns.

$C2/c$.[31] It should be noted that one-dimensional chain materials can often contain superstructures or incommensurate lattices. Structural refinements of powder data, therefore, can provide only an average structure. However, no evidence of a supercell was seen in the precession photographs. If Sr_3NiPtO_6 contains an incommensurate lattice, then it is beyond the detection limit of the X-ray methods. All attempts to refine the structure in the monoclinic space group diverged, while refinement of the Sr_3NiPtO_6 structure using the space group and atomic positions of A_4PtO_6 gave a unit cell of a = 9.5832(1) Å, c = 11.1964(1) Å and quickly converged to an R_{wp} = 14.6%, R_p = 10.8%. The observed, calculated, and difference patterns are shown in Figure 1. The structure was also refined using powder neutron diffraction data collected at the NIST Facility at Gaithersburg, MD. Although the sample contained starting material as impurities, the data were refinable to an $R_{wp} = 9.4\%$, $R_p = 7.3\%$.[36] The Sr_3NiPtO_6 structure obtained from the neutron data gave the same

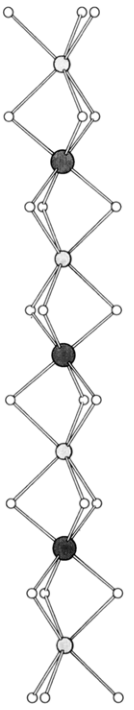

Figure 2. Single chain in the Sr_3NiPtO_6 structure: platinum (large shaded circles), nickel (small shaded circles), oxygen (open circles). The alternating PtO_6 and NiO_6 polyhedra have local O_h and D_{3h} site symmetry, respectively.

structure as that obtained from X-ray data, confirming the powder X-ray refinement.

Materials of composition Sr_3MPtO_6, M = Ni, Cu, have structures related to the one-dimensional structure of A_4PtO_6 where A = Ca, Sr, Ba. The A_4PtO_6 structure, space group $R\bar{3}c$, consists of infinite chains of alternating face-sharing PtO_6 octahedra and AO_6 trigonal prisms.[37,38] These chains are separated by the remaining electropositive elements which maintain charge balance.

In Sr_3NiPtO_6, the alkaline earth cation situated within the chains has been replaced by a first-row transition metal and, consequently, the platinum and the nickel now alternate along the infinite chain. The structure of Sr_3NiPtO_6, shown in Figure 2, consists of alternating face-sharing PtO_6 octahedra and unusual NiO_6 trigonal prisms. Figure 3 shows the complete structure viewed down the c axis. Table 2 lists the atomic positions and their esd's, and selected bond distances and angles are displayed in Table 3. The Ni–O distance of 2.17 Å is long, but Ni(II)–O distances of up to 2.26 Å have been reported: La_2NiO_4 (1.95 and 2.26 Å),[39] Y_2BaNiO_5 (1.88 and 2.19 Å).[40] The Ni–Pt distance of 2.80 Å, however, is short but still greater than the sum of the two atomic radii of 1.25 Å for Ni and 1.39 Å for Pt, suggesting no metal–metal bonding.[41]

(36) A sample containing Sr_3NiPtO_6, NiO, Pt, and SrO was refined by Rietveld analysis of powder neutron data (λ = 1.5400 Å) to R_{wp} = 9.4%, R_p = 7.3%, GOF = 1.60. Space group $R\bar{3}c$, a = 9.5932(4), c = 11.2202(5). Sr ($^2/_3$, −0.0314(2),0.5833(1)); Pt ($^1/_3$,$-^1/_3$,$^2/_3$); Ni ($^1/_3$, $-^1/_3$, 0.4167(1)); O (0.3566(3), −0.1595(3),0.5535(2)). Selected bond distances: Pt–O (2.017(2)), Pt–Ni (2.805(1)), Ni–O (2.194(2)).

(37) Randall, J.; Katz, L. *Acta Crystallogr.* **1959**, *12*, 519–521.

(38) Wilkinson, A. P.; Cheetham, A. K. *Acta Crystallogr.* **1989**, *C45*, 1672–1674.

(39) Jorgensen, J. D.; Dabrowski, B.; Pei, S.; Richards, D. R.; Hinks, D. G. *Phys. Rev. B* **1989**, *40*, 2187.

(40) Buttrey, D. J.; Sullivan, J. D.; Rheingold, A. L. *J. Solid State Chem.* **1990**, *88*, 291.

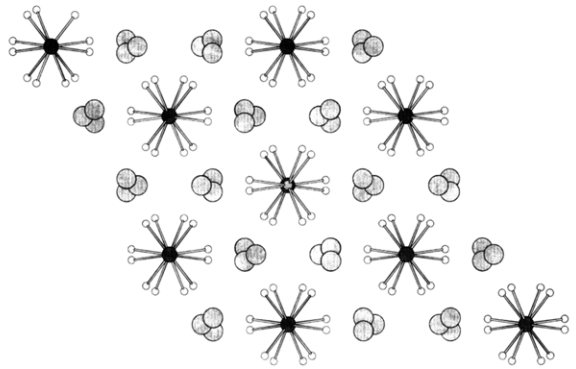

Figure 3. Structure of Sr_3NiPtO_6 looking down the *c* axis: strontium: (large shaded circles), oxygen (open circles).

Table 2. Atomic Positions of Sr_3NiPtO_6

	x	*y*	*z*
Sr	2/3	−0.0315(1)	0.5833(1)
Pt	1/3	−1/3	2/3
Ni	1/3	−1/3	0.4167(1)
O	0.3593(5)	−0.1582(5)	0.5506(35)

Table 3. Selected Bond Distances and Angles

Pt−O (×6)	2.037(4)
Pt−Ni (×2)	2.799(4)
Ni−O (×6)	2.170(4)
Sr−O (×2)	2.590(4)
Sr−O (×2)	2.752(5)
Sr−O (×2)	2.464(4)
Sr−O (×2)	2.683(4)
O−Pt−O (×6)	83.68(16)
O−Pt−O (×6)	96.32(16)
O−Pt−O (×3)	180.0

The structure is isotypic with the known one-dimensional chain compound Sr_3CuPtO_6.[31] In the case of Sr_3CuPtO_6, the strong preference of Cu(II) to bond in square-planar coordination moves the copper from the center to near a face of the trigonal prism, distorting the structure and lowering the symmetry to *C*2/*c*. The platinum still retains its octahedral coordination.

Magnetic Characterization. *Sr_3NiPtO_6 and Sr_3CuPtO_6*: Magnetic susceptibility studies of polycrystalline Sr_3NiPtO_6 in fields of 1, 5, and 40 kG indicate an onset of magnetic ordering at ~25 K as shown in Figure 4. The susceptibilities in different fields are all qualitatively similar. The magnetic behavior of Sr_3NiPtO_6 is characteristic of many linear chain materials.[42−44] At low temperatures, the susceptibility decreases and flattens indicating an order−disorder transition associated with an antiferromagnetic transition. Since Sr_3NiPtO_6 is insulating, this antiferromagnetic coupling must be due to superexchange or dipole−dipole interactions. The increase in susceptibility at 4 K is presumably due to paramagnetic impurities. The susceptibility data also suggest the presence of only short-range ordering in this system since the susceptibility does not "turn over" as in other antiferromagnets. Powder neutron diffraction studies of the Sr_3NiPtO_6 at 10 K gave the same diffraction pattern as that obtained at room temperature with no magnetic peaks, confirming the absence of long range order. We have attempted

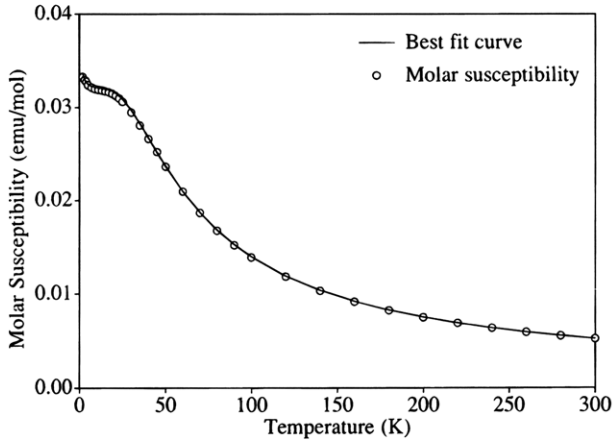

Figure 4. Magnetic susceptibility as a function of temperature of Sr_3NiPtO_6 at 5 kG. The best fit of data to our model, shown as the solid line, gave $D = 90.2$ K, $g = 2.37$, $\chi_{TIP} = 5.7 \times 10^{-4}$ emu/mol, and $C = 0.004$ emu K/mol. The leveling of the susceptibility at ~25 K indicates the onset of antiferromagnetic ordering.

to fit the susceptibility data to an $S = 1$ one-dimensional Heisenberg antiferromagnetic model[45,46] with a paramagnetic correction for the impurities, but the fit was poor. A Curie-Weiss fit of the susceptibility above 50 K yielded $\theta = -14.1$ K and 3.35 μ_B/mol of Sr_3NiPtO_6. A spin-only value of 2.83 μ_B (equivalent to two unpaired electrons) would be expected for trigonal prismatic Ni(II), d^8, and low-spin octahedral Pt(IV), d^6. Ni(II) oxides, however, typically exhibit magnetic moments near 3.2 μ_B due to spin−orbit coupling.[47]

As mentioned earlier, $S = 1$ one-dimensional chain systems have attracted much attention recently because they can possess an unusual quantum phenomenon known as the Haldane gap.[29,30] Sr_3NiPtO_6 is a one-dimensional system with $S = 1$. However, in our system, there is no evidence, such as a turnover in magnetic susceptibility at low temperatures, of a gap. The absence of a Haldane gap could be due to high single-ion anisotropy of the magnetic centers in addition to low coupling exchange.[48] Also, Sr_3NiPtO_6 contains alternating Ni(II) ($S = 1$) and Pt(IV) ($S = 0$) along the chain, while all reported Haldane systems have contained chains with uniform Ni(II) magnetic centers.[26−28,48,49]

Taking these factors into account, we have attempted to fit the magnetic susceptibility of Sr_3NiPtO_6 to a model which contains high single-ion anisotropy and very small coupling exchange.[50] Our best fit gave a single-ion anisotropy parameter, *D*, of 90.2 K, $g = 2.37$, a temperature-independent paramagnetic value, χ_{TIP}, of 5.7×10^{-4} emu/mol, and $C = 0.004$ emu K/mol from the Curie-law contribution from paramagnetic impurities. Thus, based on our fit, Sr_3NiPtO_6 is structurally a chain, however its magnetic properties are best described as those of isolated Ni(II) ions with large *D* and a small amount of paramagnetic impurities. The

(41) Shannon, R. D.; Prewitt, C. T. *Acta Crystallogr.* **1969**, *B25*, 925.
(42) de Jongh, L. J.; Miedema, A. R. *Adv. Phys.* **1974**, *23*, 1.
(43) Carlin, R. L. *Magnetochemistry*; Springer-Verlag: Berlin, 1986.
(44) Carlin, R. L. *J. Chem. Educ.* **1991**, *68*, 361−364.
(45) Bonner, J. C.; Fisher, M. E. *Phys. Rev.* **1964**, *135*, 640.
(46) Greaney, M. A.; Ramanujachary, K. V.; Teweldemedhin, Z.; Greenblatt, M. *J. Solid State Chem.* **1993**, *107*, 554.
(47) Figgis, B. N. *Introduction to Ligand Fields*; Interscience Publishers: New York, 1966.
(48) Renard, J. P.; Clement, S.; Verdaguer, M. *Proc. Indian Acad. Sci. (Chem. Sci.)* **1987**, *98*, 131.
(49) Ajiro, Y.; Goto, T.; Kikuchi, H.; Sakakibara, T.; Inami, T. *Phys. Rev. Lett.* **1989**, *63*, 1424.

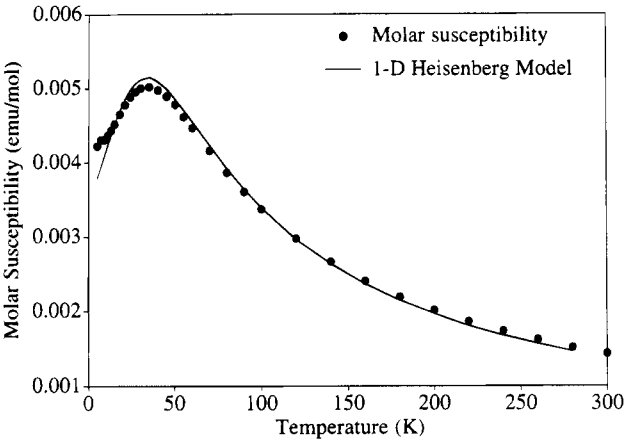

Figure 5. Magnetic susceptibility as a function of temperature of Sr_3CuPtO_6 at 5 kG. The curve shows the best fit to the $S = {}^1/_2$ Heisenberg linear chain model, with $J/k = -26.1$ K and $g = 2.21$.

Ni ions are able to couple slightly antiferromagnetically at low temperatures as indicated by the leveling in the susceptibility; this exchange, however, is only short range in nature, which is supported by the low-temperature neutron studies.

In contrast, the susceptibility of Sr_3CuPtO_6, shown in Figure 5, clearly displays antiferromagnetic ordering. Sr_3CuPtO_6 has an ordering temperature of ~40 K, and the turnover in the susceptibility curve at low temperatures indicates the presence of quasi-long-range order. The broadness of the magnetic transition is consistent with the low-dimensional nature of the structure, since a three-dimensional structure would be expected to have a cusp-shaped transition, indicating spontaneous, long-range order. A Curie–Weiss law fit of the data above 100 K gave $\theta = -46.6$ K and a magnetic moment typical of Cu(II) of 1.99 μ_B/mol of Sr_3CuPtO_6. This value is in reasonable agreement with the spin-only value of 1.73 μ_B expected for one unpaired electron of square planar Cu(II), d^9, and no unpaired electrons in low-spin, octahedral Pt(IV), d^6.

Since Cu(II) is typically a Heisenberg ion,[43] the susceptibility of Sr_3CuPtO_6 was fitted to an $S = {}^1/_2$ Heisenberg linear chain model (Figure 5).[51] The least-squares fit gave an exchange constant of $J/k = -26.1$ K and a powder average g value of 2.21. The powder g value obtained by electron paramagnetic resonance is 2.15. Using g value of 2.21, the expected magnetic moment for one unpaired electron is 1.91 μ_B, which is close to the value of 1.99 μ_B obtained from the susceptibility data fit.

The iridium analogs, Sr_3NiIrO_6 and Sr_3CuIrO_6,[52] as well as Sr_3CoPtO_6 and Sr_3ZnIrO_6, have also been prepared. Preliminary experiments show complex magnetic behaviors in these systems, and the results will be published shortly.

Summary

Single crystals of a new Sr_3NiPtO_6 were synthesized by electrolysis in molten KOH. The structure was determined by Rietveld analysis of powder X-ray and neutron diffraction data. Sr_3NiPtO_6 is isotypic with the linear chain material Sr_3CuPtO_6. Magnetically, Sr_3NiPtO_6 contains isolated Ni(II) ions with large single-ion anisotropy and exhibits short range antiferromagnetic ordering at ~25 K. Sr_3CuPtO_6 was found to be a well-behaved one-dimensional Heisenberg antiferromagnet.

Acknowledgment. We are indebted to T. Jolicoeur and O. Golinelli for the fit of the Sr_3NiPtO_6 magnetic data and to P. Lee for many useful discussions. We also thank J. Stallick for collecting the neutron data. This work was supported by the Massachusetts Institute of Technology, Center for Materials Science and Engineering under Grant DMR 9022933.

Supplementary Material Available: Powder neutron Rietveld refinement data and tables of positional parameters and anisotropic thermal parameters (63 pages). Ordering information is given on any current masthead page.

(50) Jolicoeur, T.; Golinelli, private communication. The Hamiltonian for the single-ion approximation is given as $\hat{\mathbf{H}}_{S.I.} = D\sum_n(\mathbf{S}_n^z)^2$, where D is the single-ion anisotropy parameter. Assuming no coupling between magnetic centers, $\hat{\mathbf{H}}_{S.I.} = J\sum_n(\hat{\mathbf{S}}_n\cdot\hat{\mathbf{S}}_{n+1})$ is negligible. For $\mathbf{H}_{S.I.}$

$$\frac{1}{g^2\mu_B{}^2}\chi^z(T) = \frac{2\beta}{2 + e^{\beta D}}$$

where $\beta = 1/T$

$$\frac{1}{g^2\mu_B{}^2}\chi^x(T) = \frac{2}{D}\frac{1 - e^{-\beta D}}{1 + 2e^{-\beta D}}$$

Neglecting g anisotropy

$$\chi_{measured} = {}^1/_3(\chi^z + 2\chi^x)$$

$$\frac{1}{g^2\mu_B{}^2}\chi_{measured} = {}^1/_3\left(2\beta + \frac{4}{D}(e^{\beta D} - 1)\right)\frac{1}{2 + e^{\beta D}}$$

The best fit is given as

$$\chi = g^2\mu_B{}^2F(D,\beta) + \chi_{TIP} + C/T$$

where $F(D,\beta) = {}^1/_3(2\beta + (4/D)(e^{\beta D} - 1))1/(2 + e^{\beta D})$, χ_{TIP} is the temperature-independent paramagnetism, and C/T is the Curie-law contribution from paramagnetic impurities.

(51) Hatfield, W. E. *J. Appl. Phys.* **1981**, *52*, 1985–1990.
(52) Neubacher, M.; Muller-Buschbaum, H. *Z. Anorg. Allg. Chem.* **1992**, *607*, 124.